

Supplementary Information for

Designed synthesis of Zr-based ceria-zirconia-neodymia composite with highly thermal stability and its enhanced catalytic performance for Rh-only three-way catalyst

Su-Ning Wang^a, Jian-Li Wang^{b,c}, Wei-Bo Hua^a, Meng-Meng Sun^d, Zhong-Hua Shi^{b,c}, Shan-Dong Yuan^d, Lin Zhong^a, Yao-Qiang Chen^{,a,b,c,d}*

^a College of Chemical Engineering, Sichuan University, Chengdu, Sichuan 610064, China.

^b Key Laboratory of Green Chemistry & Technology, Ministry of Education, College of Chemistry, Sichuan University, Chengdu, Sichuan 610064, China.

^c Center of Engineering of Environmental Catalytic Material, Chengdu, Sichuan 610064, China.

^d Institute of New Energy and Low-carbon Technology, Sichuan University, Chengdu, Sichuan 610064, China.

**Corresponding author. Email: nic7501@scu.edu.cn (Prof. Dr. Yao-Qiang Chen)*

This Supplementary Information includes:

Table S1. BET surface area for several advanced ceria-zirconia mixed oxides with different preparation methods and thermal treatment.

Table S2. Structural parameters of samples calcined at different temperatures.

Table S3. The reduction peak temperatures and quantitative analysis results of H₂-TPR for the samples.

Table S4. The quantitative analysis results of OSC for the samples and the surface atomic ratios of Zr/Ce and Ce³⁺ in Ce (%) derived from XPS analyses.

Table S5. The OSC for the samples pretreated in H₂ flowing at 950 °C for 1 h.

Table S6. Light-off temperatures ($T_{50\%}$) of NO, CO and C₃H₈ over catalysts.

Figure S1. TG/DTG/DSC curves of CZ/N235-70.

Figure S2. XRD diffraction patterns of dried precipitates, fresh samples and aged samples.

Figure S3. The illustrative crystallographic structure of cubic Ce_{0.6}Zr_{0.4}O₂.

Figure S4. Multiples of crystal growth for the fresh and aged samples based on the corresponding crystallite size for dried materials.

Figure S5. Raman spectra of dried precipitates, fresh samples and aged samples.

Figure S6. The statistics of particle distribution of CZ/N235-600 (a) and CZ-600 (b).

Figure S7. FTIR spectra of samples treated at different temperatures.

Figure S8. H₂-TPR profiles of the sample calcinated at 600 and 1000 °C.

Figure S9. H₂-TPR profiles of the fresh and aged catalysts.

Figure S10. OSC values of the fresh and aged catalysts.

Figure S11. Rh dispersions of the fresh and aged catalysts.

Figure S12. Rh 3d XPS spectra of the fresh and aged catalysts.

Table S1. BET surface area for several advanced ceria-zirconia mixed oxides with different preparation methods and thermal treatment.

Structure	Preparation method	Thermal treatment	Surface area (m ² ·g ⁻¹)	Reference
Ce _{0.15} Zr _{0.85} O ₂	Co-precipitation combined with mechanical mixing of N235	600 °C/3 h in air	92	This work
		1000 °C/5 h in air	31	
Ce _{0.15} Zr _{0.85} O ₂	Co-precipitation	600 °C/3 h in air	71	This work
Ce _{0.18} Zr _{0.82} O ₂		1000 °C/5 h in air	13	
Ce _{0.65} Zr _{0.35} O ₂	Continuous hydrothermal synthesis in supercritical water	700 °C/5 h in air	92	Reference [2]
		1000 °C/6 h in H ₂ and 1000 °C/6 h in O ₂	20	
Ce _{0.2} Zr _{0.8} O ₂	Co-precipitation method combined with supercritical drying technology	500 °C in air	97	Reference [20]
		1100 °C/4 h in air	28	
Ce _{0.68} Zr _{0.32} O ₂	CTAB-assisted precipitation technique	900 °C/2 h in air	40	Reference [30]

Ce-Zr-Pr-O ₂ (Ce/Zr=1/8)	Conventional co-precipitation method	500 °C/4 h in air	100	Reference [19]
		1100 °C/4 h in air	10	
Ce _{0.67} Zr _{0.33} O ₂	Co-precipitation and supercritical drying method	600 °C/4 h in air	55	Reference [15]
		1100 °C/4 h in air	8	
CeZr ₂ O _x	Homogeneous precipitation method	500 °C/3 h in air	107	Reference [5]

Table S2. Structural parameters of samples calcined at different temperatures.

Sample	Crystal form	Crystallite size (Å)	Weight (%)	$a = b$ (Å)	c (Å)	V (Å ³)	R_{wp} (%)
CZ-70	c -Ce _{0.6} Zr _{0.4} O ₂	29	-	5.307	5.307	149.468	-
CZ/N235-70	c -Ce _{0.6} Zr _{0.4} O ₂	33	-	5.308	5.308	149.552	-
CZ-600	t -Ce _{0.15} Zr _{0.85} O ₂	81	100	3.644	5.209	69.169	8.45
CZ/N235-600	t -Ce _{0.15} Zr _{0.85} O ₂	69	100	3.648	5.219	69.454	7.80
CZ-1000	t -Ce _{0.18} Zr _{0.82} O ₂	154	94.6	3.686	5.213	70.827	6.76
	t -ZrO ₂		5.4	3.653	5.202	69.418	
CZ/N235-1000	t -Ce _{0.15} Zr _{0.85} O ₂	125	100	3.649	5.228	69.612	8.26

Table S3. The reduction peak temperatures and quantitative analysis results of H₂-TPR for the samples.

Sample	Temperature of reduction peak (°C)	Total H ₂ consumption (μmol·g ⁻¹)	Reduction ratio (%) ^a
CZ-600	583	405	70.43
CZ/N235-600	563	422	73.39
CZ-1000	699	334	58.09
CZ/N235-1000	585	380	66.09

a: The ratio between experimental total H₂ consumption and the theoretical H₂ consumption which is calculated assuming that all Ce species are in oxidized state (Ce⁴⁺) before H₂-TPR test and can be totally reduced to Ce³⁺.

Table S4. The quantitative analysis results of OSC for the samples and the surface atomic ratios of Zr/Ce and Ce³⁺ in Ce (%) derived from XPS analyses.

Sample	OSC ($\mu\text{mol}\cdot\text{g}^{-1}$)	OSC (mol O ₂ /mol CeO ₂)	Oxidation ratio (%) ^b	Zr/Ce	Ce ³⁺ in Ce (%)
CZ-600	132	0.1148	45.92	5.64	16.92
CZ/N235-600	143	0.1243	49.72	5.62	23.80
CZ-1000	74	0.0643	25.72	6.29	11.70
CZ/N235-1000	138	0.1200	48.00	5.69	21.77

b: The ratio between experimental OSC (expressed as mol O₂/mol CeO₂) and the theoretical OSC value (0.25 mol O₂/mol CeO₂).

Table S5. The OSC for the samples pretreated in H₂ flowing at 950 °C for 1 h.

Sample	OSC ($\mu\text{mol}\cdot\text{g}^{-1}$)
CZ-600	218
CZ/N235-600	260
CZ-1000	173
CZ/N235-1000	245

Table S6. Light-off temperatures ($T_{50\%}$) of NO, CO and C₃H₈ over catalysts.

Catalyst	NO	CO	C ₃ H ₈
	$T_{50\%}$ (°C)	$T_{50\%}$ (°C)	$T_{50\%}$ (°C)
Rh/CZ-f	204	205	347
Rh/CZ/N235-f	168	171	278
Rh/CZ-a	278	280	-
Rh/CZ/N235-a	229	235	-

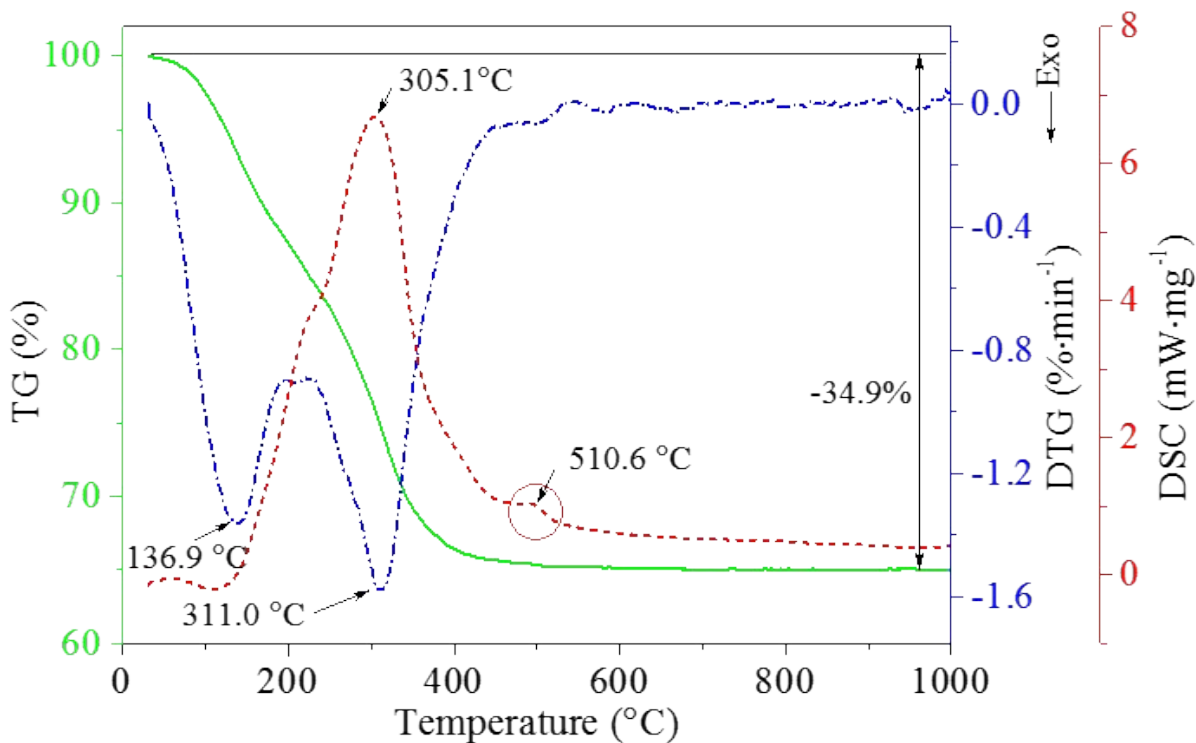


Figure S1. TG/DTG/DSC curves of CZ/N235-70.

Figure S1 shows the TG/DTG/DSC curves of the CZ/N235-70. A weight loss of 34.9 % is calculated from TG characterization between room temperature and 1000 °C. It can be found that DTG curve displays two mass loss stages, corresponding with peaks located at about 136.9 and 311.0 °C, respectively. The peak observed at 136.9 °C could be attributed to the loss of water. While a stronger plateau at approximately 311.0 °C is probably assigned to the decomposition of carbonates, hydroxides and organics, which is coincident with the endothermic peak found in DSC profile. The other endothermic peak centered at about 510.6 °C is not associated with weight loss, suggesting the phase transformation of materials.

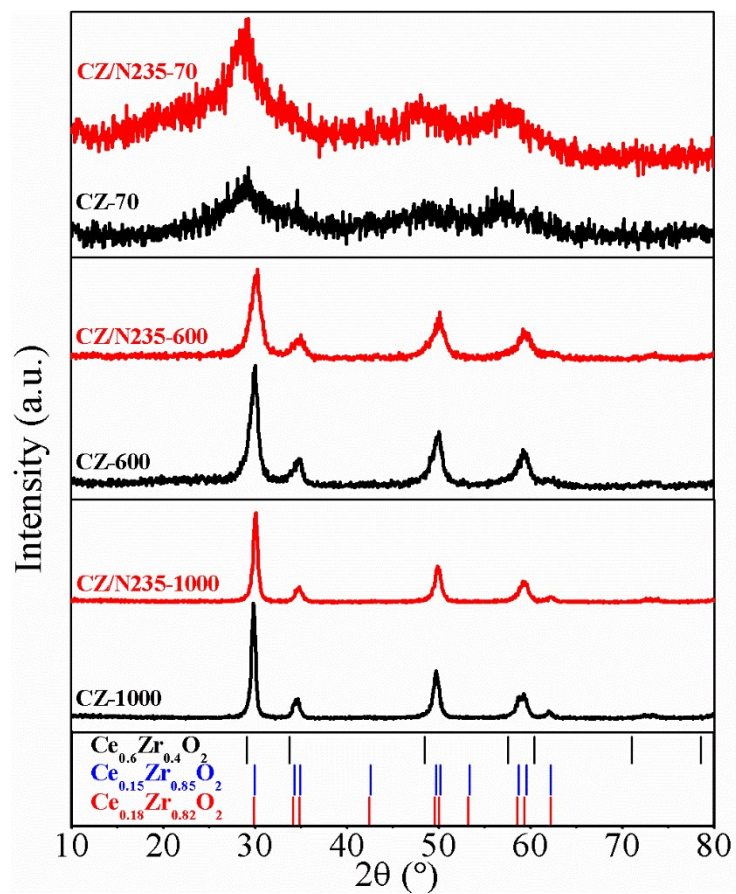


Figure S2. XRD diffraction patterns of dried precipitates, fresh samples and aged samples.

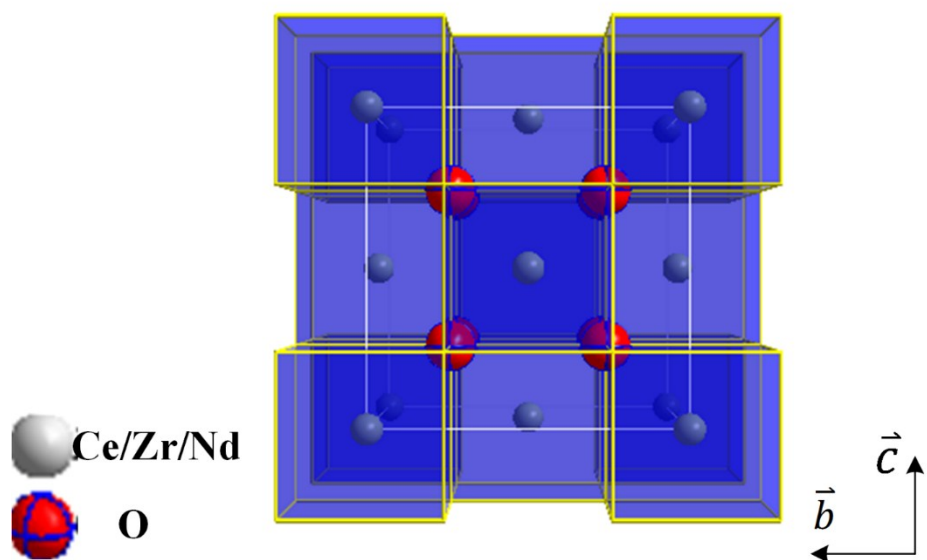


Figure S3. The illustrative crystallographic structure of cubic $\text{Ce}_{0.6}\text{Zr}_{0.4}\text{O}_2$.

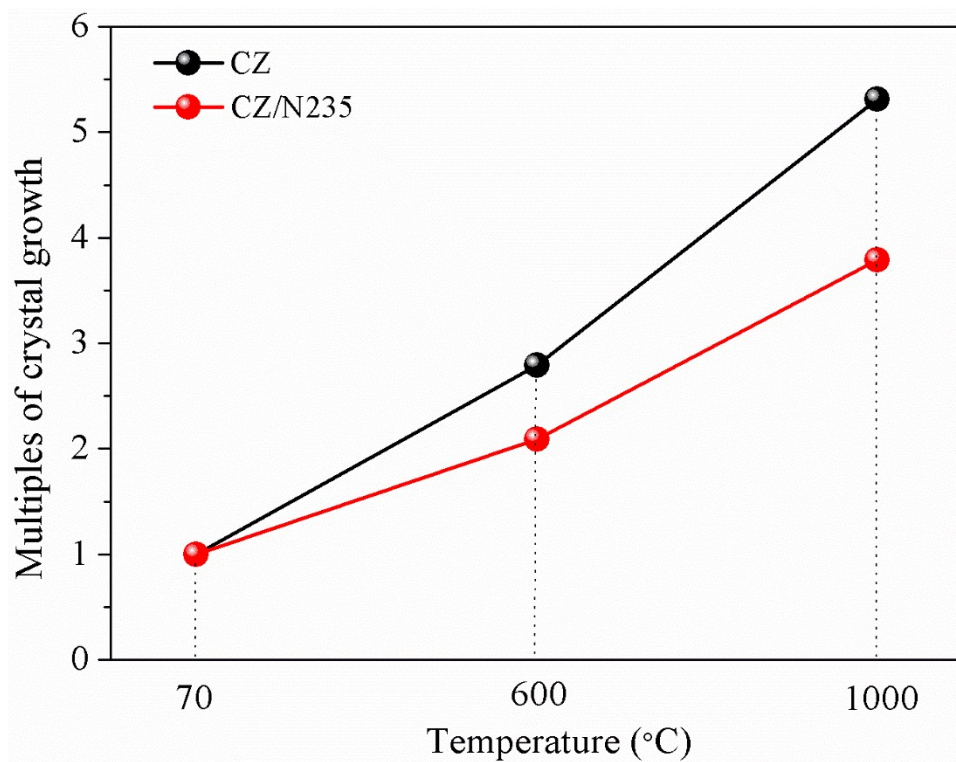


Figure S4. Multiples of crystal growth for the fresh and aged samples based on the corresponding crystallite size for dried materials.

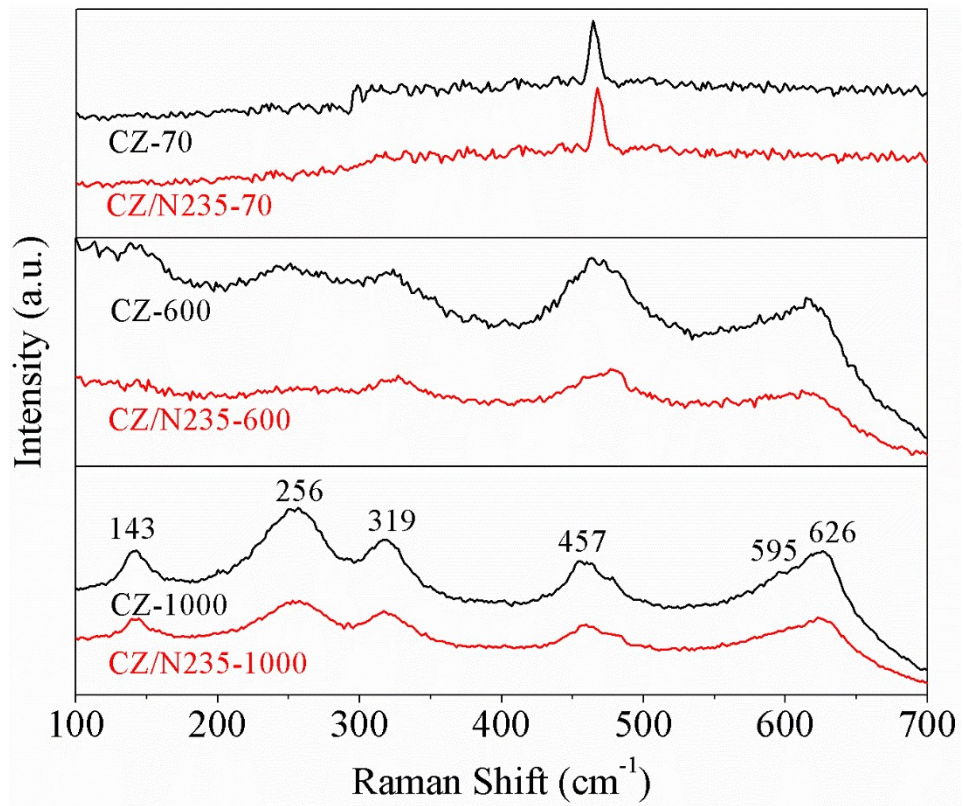


Figure S5. Raman spectra of dried precipitates, fresh samples and aged samples.

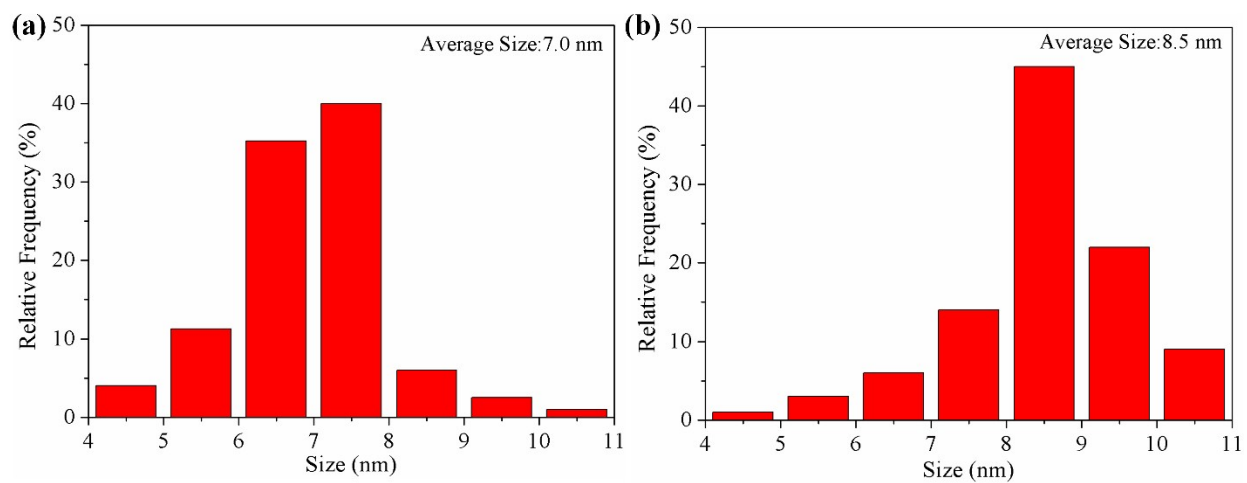


Figure S6. The statistics of particle distribution of CZ/N235-600 (a) and CZ-600 (b).

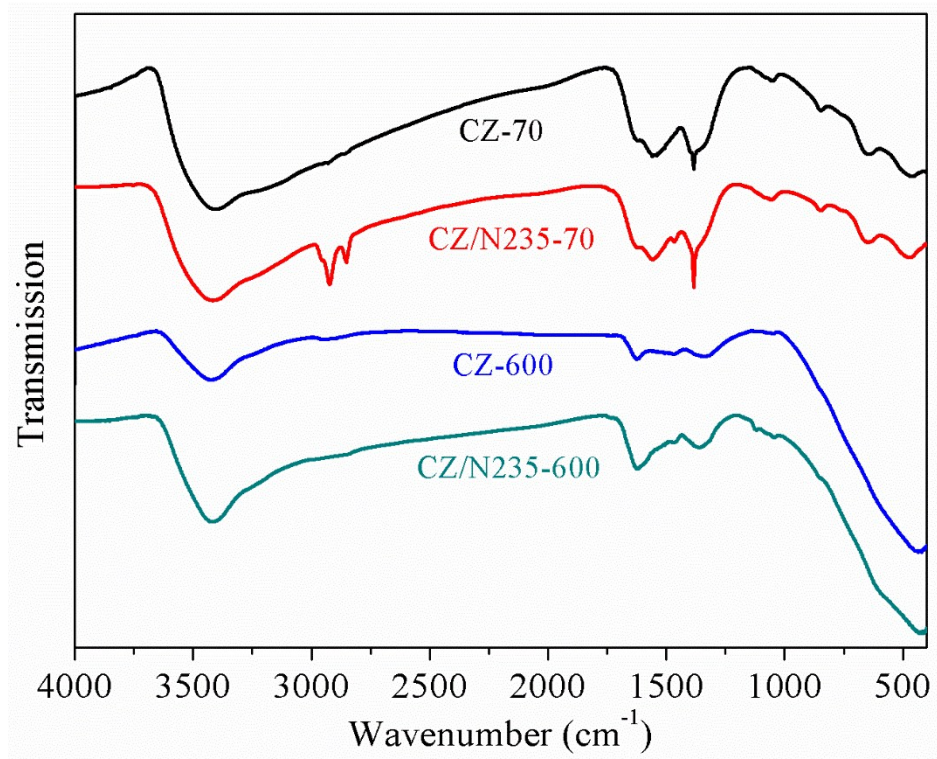


Figure S7. FTIR spectra of samples treated at different temperatures.

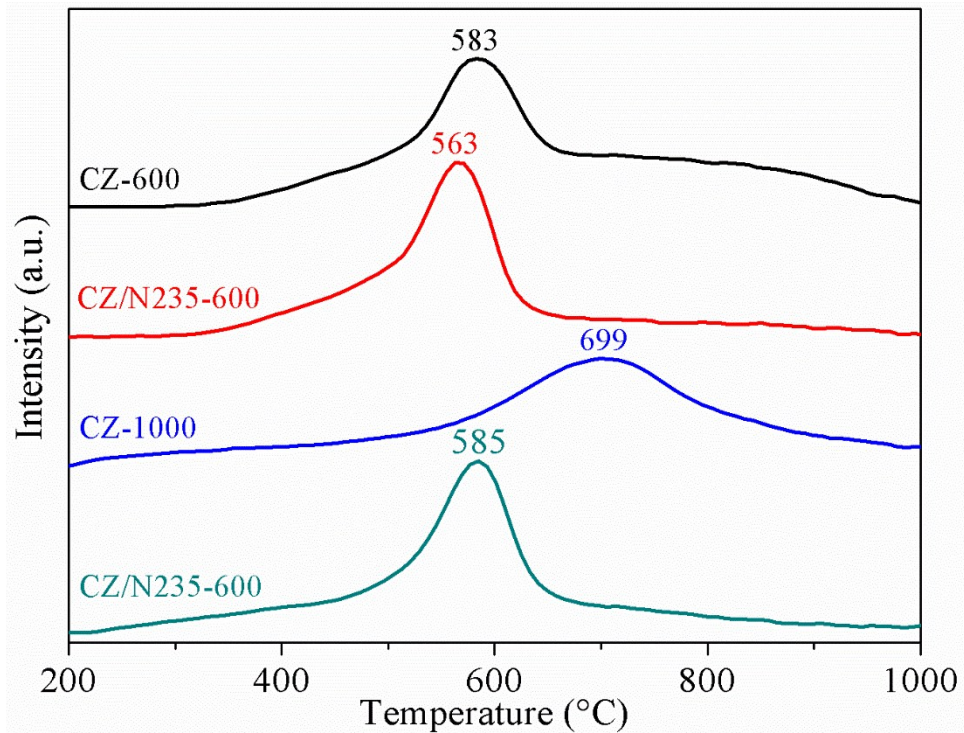


Figure S8. H₂-TPR profiles of the sample calcinated at 600 and 1000 °C.

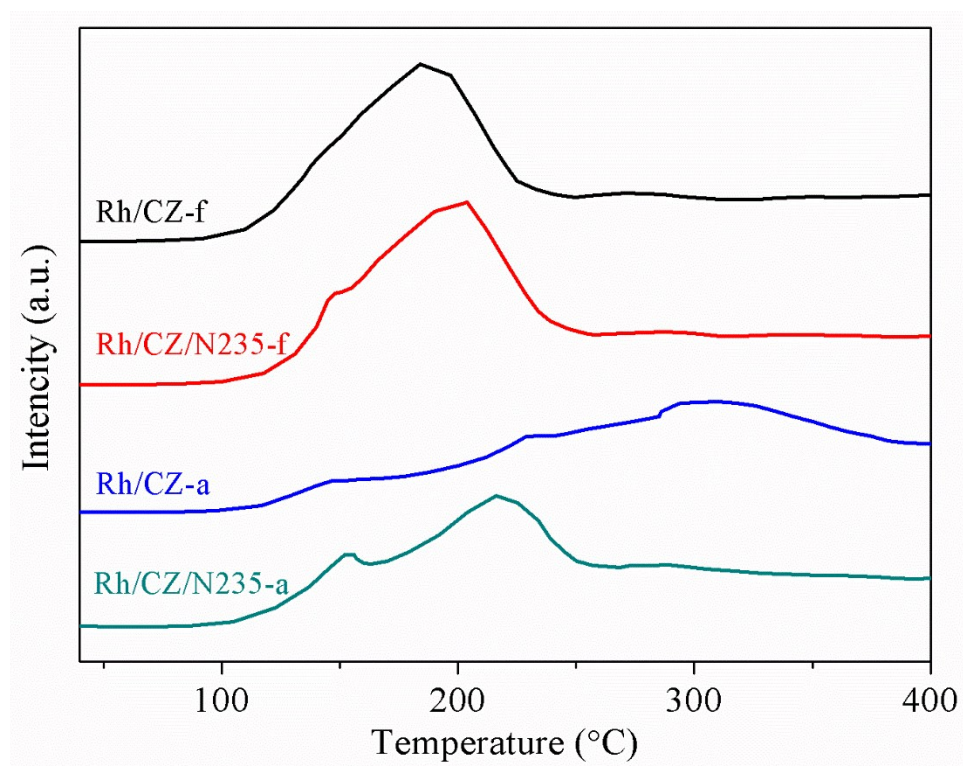


Figure S9. H₂-TPR profiles of the fresh and aged catalysts.

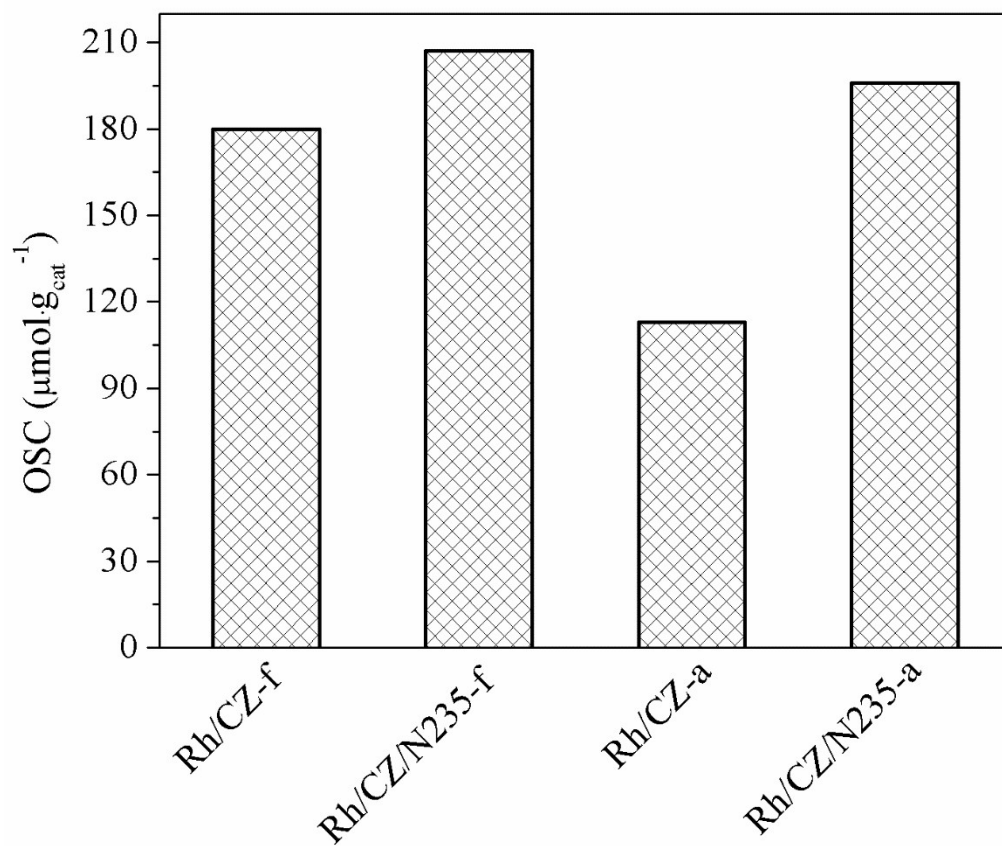


Figure S10. OSC values of the fresh and aged catalysts.

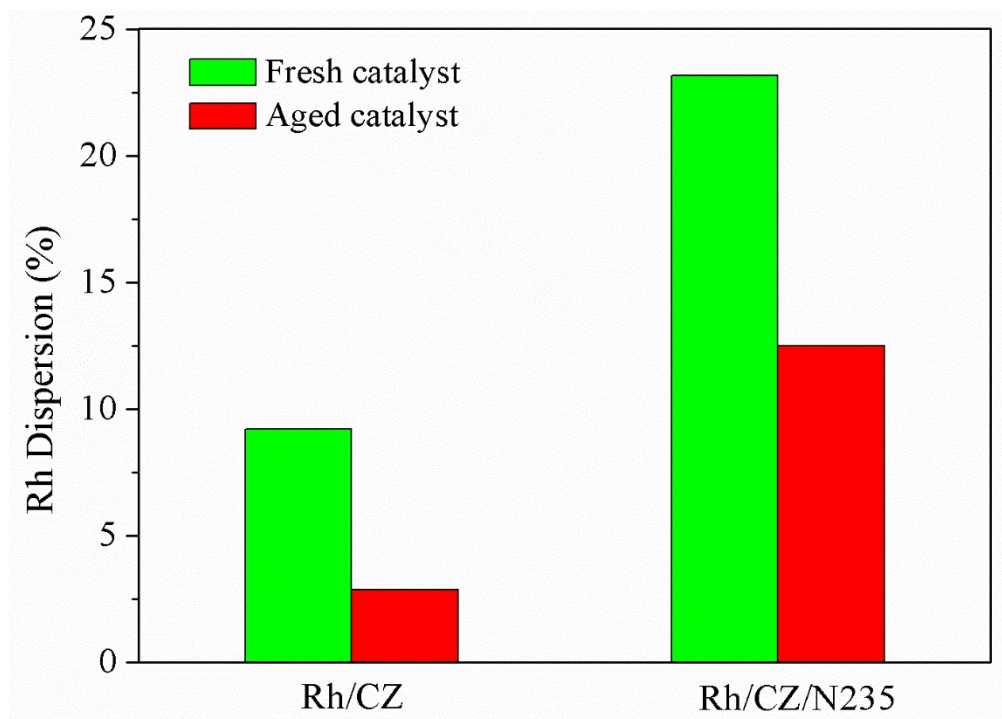


Figure S11. Rh dispersions of the fresh and aged catalysts.

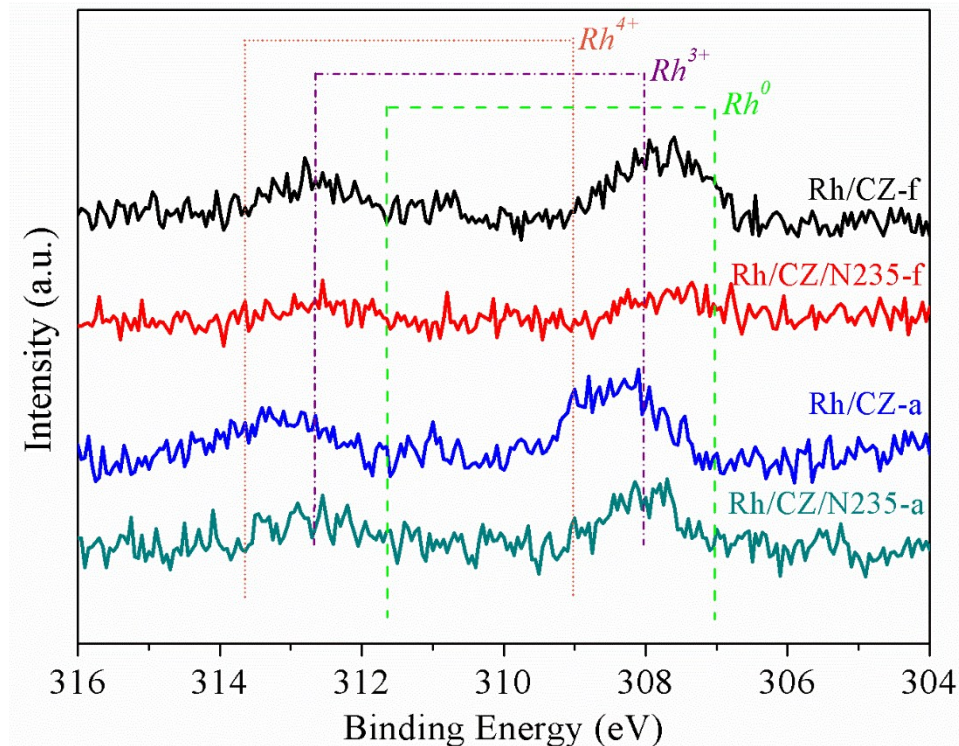


Figure S12. Rh 3d XPS spectra of the fresh and aged catalysts.

The spectra of Rh ($3d_{5/2}$, $3d_{3/2}$) for fresh and aged catalysts are shown in Figure S12. For fresh catalysts, faint peaks attributed to Rh^0 are detected in a fashion at approximately 307 eV, demonstrating the presence of slight metallic Rh. Prominent peaks at about 308 eV ($Rh\ 3d_{5/2}$) could be observed, which is in accordance with the literature data for Rh_2O_3 .^{1,2} Upon aging treatment, the peaks of $Rh\ 3d_{5/2}$ are shifted to higher binding energies, especially Rh/CZ-a, indicating the formation of more RhO_2 on the surface of Rh/CZ-a.³ According to the references,³⁻⁵ the presence of RhO_2 , which is hard to reduce to the active state, will result in deteriorated catalytic property for the aged catalysts. So Rh/CZ/N235-a may have a superior catalytic performance due to its lower amount of RhO_2 .

References

1. K. Dohmae, T. Nonaka and Y. Seno, *Surf. Interface Anal.*, 2005, **37**, 115-119.
2. Z. Weng-Sieh, R. Gronsky and A.T. Bell, *J. Catal.*, 1997, **170**, 62-74.
3. S. Suhonen, M. Valden, M. Hietikko, R. Laitinen, A. Savimäki and M. Härkönen, *Appl. Catal., A*, 2001, **218**, 151-160.
4. U. Lassi, R. Polvinen, S. Suhonen, K. Kallinen, A. Savimäki, M. Härkönen, M. Valden and R. L. Keiski, *Appl. Catal., A*, 2004, **263**, 241-248.
5. B. Zhao, R. Ran, Y. Cao, X. Wu, D. Weng, J. Fan and X. Wu, *Appl. Surf. Sci.*, 2014, **308**, 230-236.